Electronic Supplementary Material (ESI) for Green Chemistry.
This journal is © The Royal Society of Chemistry 2022

Supplementary Information

Pathways of ammonia electrooxidation on nickel hydroxide anodes and an alternative route towards recycled fertilizers

Jury J. Medvedev,[a] Yulia Tobolovskaya,[a] Xenia V. Medvedeva,[a] Stephen W. Tatarchuk,[a] Feng Li,[a] Anna Klinkova,*[a]

[a]*Department of Chemistry, University of Waterloo, 200 University Avenue West, Waterloo, Ontario N2L 3G1, Canada.*

*Corresponding Author: aklinkova@uwaterloo.ca

13 Pages, 12 Figures, and 4 Tables are included

Details of the assessment of waste-ammonia-to-fertilizer recovery strategies.

To assess the potential of the electrochemical ammonia-to-fertilizer approach, we compared a roughly estimated gross profit from the electrochemical production of fertilizer to that from the chemical process that is currently used in some anaerobic digestors.

The gross profit was calculated as

$$\delta = \alpha_{out} - \alpha_{in} \quad \text{(S1)},$$

where δ is the simplified gross profit from the fertilizer production from 1 kg of waste-ammonia (in USD), α_{out} is the cost of produced fertilizer, and α_{in} is the cost of chemicals/electrolytes that are needed for the processes. The amounts of precursors needed for the process were calculated based on corresponding chemical equations S2-S4. Equation S2 and S3 correspond to the acid-base reaction between ammonia and inorganic acids used for in chemical approach, whereas equation S3 correspond to the electrochemical conversion of ammonia into NH_4NO_3. The numbers in brackets show the concentration of precursor used in for the calculations. We note, that 0.1 M K_2SO_4 and 0.1 M K_2HPO_4 were considered as electrolytes for electrochemical approach.

$2\ NH_3\ \mathit{(0.3M)} + H_2SO_4\ \mathit{(0.15\ M)} \rightarrow (NH_4)_2SO_4$ (S2)

$NH_3\ \mathit{(0.3M)} + HNO_3\ \mathit{(0.3\ M)} \rightarrow NH_4NO_3$ (S3)

$2\ NH_3\ \mathit{(0.3\ M)} + 3\ H_2O \rightarrow NH_4NO_3 + 4H_2$ (S4)

The cost of NH_3-containing wastewater is omitted due to being equal in all strategies. Capital costs and profits from co-production of hydrogen are not considered.

For the calculation of α_{in} and α_{out}, we used available market prices of chemical compounds, which are summarized in Table S1.

Table S1. Market price of raw materials[1,2]

Raw materials / Electrolytes	ECHEMI[a] Market price ($ kg^{-1})	INTRATEC[b] US ($ kg^{-1})
H_2SO_4	0.12	0.05
HNO_3	0.47	0.26
$(NH_4)_2SO_4$	0.44	0.17
NH_4NO_3	0.55	0.25
K_2SO_4	0.70	0.37
K_2HPO_4	1.31	–[c]

[a] The current prices of chemical were taken from https://www.echemi.com/. The values correspond to the prices available on Aug 2021. We note that the prices may vary depending on the year, supplier, etc. [b] The values were taken from https://www.intratec.us and represent historical prices of the chemicals in 2007. [c] The information was not available.

The relative prices of chemicals retrieved from two databases are shown in Figure S1. Notably, although the actual current prices (data from the Echemi database) are almost twice higher than the historical prices in 2007 (data from the Intratec database), the relative prices of the chemicals are very close.

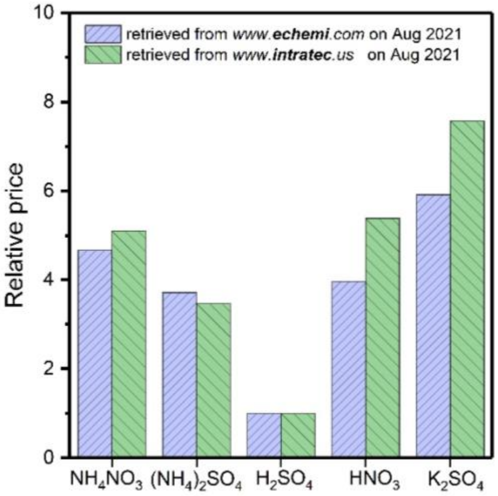

Figure S1. Relative prices of chemicals retrieved from *Echemi* and *Intratec* databases (obtained by dividing the price of each chemical by the price of H_2SO_4, which has the lowest price among these five chemicals).

Table S2. Assessment of several waste-ammonia-to-fertilizer recovery strategies.

Strategy	Reaction	α_{in} ($)	Produced fertilizer	N-P-K-(S)	α_{out} ($)	δ ($)
Acid-base reaction	**$2NH_3$ (0.3M) + H_2SO_4 (0.15M) → $(NH_4)_2SO_4$ (0.15M)**	**0.15**	**$(NH_4)_2SO_4$**	**21-0-0-(24)**	**0.66**	**0.51**
Acid-base reaction	**NH_3 (0.3M) + HNO_3 (0.3M) → NH_4NO_3 (0.3M)**	**1.00**	**NH_4NO_3**	**35-0-0-(0)**	**1.18**	**0.18**
Electrolysis in 0.1M K_2SO_4	**$2NH_3$ (0.3M) + $3H_2O$ → NH_4NO_3 (0.15M) + $4H_2$**	**1.90**	**NH_4NO_3 +K_2SO_4 (3:2)**	**14-0-32-(11)**	**2.49**	**0.59**

α_{in}: cost of acids/electrolytes to treat 1 kg of NH_3 (based on INTRATEC)[2]

α_{out}: price of fertilizer derived from 1 kg of NH_3 (based on INTRATEC)[2]

$\delta = \alpha_{out} - \alpha_{in}$: simplified gross profit from the fertilizer produced by treating 1kg of NH_3 following different strategies. The cost of NH_3-containing wastewater is omitted due to being equal in all strategies. Capital costs and profits from co-production of hydrogen are not considered (see the discussion in the text).

Performance of different Ni-based electrocatalysts towards electrochemical ammonia oxidation

Table S3. AOR performance of selected electrocatalysts[3-11]

Anode	E or *J*	pH	Electrolyte	Results	Ref.
$Ni_{98}Pd_2$	20 mA cm^{-2}	10.5	0.2 M NH_4NO_3 **+ 1 M $NaNO_3$**	**$FE_{(N2)}$ 38.7%**	[3]
NF[a]	0.7 $V_{Hg/HgO}$	11	20 ppm NH_3 + **0.1 M Na_2SO_4**	**$FE_{(N2)}$ 50%**	[4]
NF[a]	0.85 $V_{Hg/HgO}$	11	20 ppm NH_3 + **0.1 M Na_2SO_4**	**$FE(NO_3^-)$ 10%**	[4]
Activated Ni	20 mA cm^{-2}	11	50 mM NH_4ClO_4 + **1 M $NaClO_4$**	No FEs are given. **3:1 N_2/NO_3^- ratio**	[5]
Ni_2P/NF	15 mA[b]	13	1000 ppm NH_3 **+ 0.1 M KOH**	Up to 50% CE without specification (**N_2 major; NO_2^-, NO_3^- ~ 1:1**)	[6]
$Ni_xCu_{1-x}(OH)_2$	1.53 V_{RHE}	13	1 mM NH_3 **+ 0.1 M KOH**	>**80% FE of NO_2^-** minor oxidation of NH_3 was observed without applied voltage	[7]
CNT-Ni[c]	1.5 V_{RHE}	11	130 ppm NH_3 **+ 10mM Na_2SO_4**	No FE are given. ~ 1**4:1 N_2/ NO_3^- ratio**	[8]
CNS-Ni[d]	1.5 V_{RHE}	11	130 ppm NH_3 **+ 10mM Na_2SO_4**	No FE are given. ~ 1**6:1 N_2/ NO_3^- ratio**	[8]
CuCo/NF	1.1 $V_{Ag/AgCl}$	11	450 ppm NH_3 **+ 10mM Na_2SO_4**	Up to 80% (4:1 **N_2/ NO_3^- ratio**)	[9]
NiO NPs	30 mA cm^{-2}	9	200 mM NH_4OH **+ 100mM $NaNO_3$**	No FE are given. **N_2 major**. **NO_2^-: NO_3^-** ~ 1:2	[10]
NiO NPs/NF	2 mA cm^{-2}	9	100 ppm NH_3 **+ 0.1M Na_2SO_4**	80% removal; 90% **N_2** selectivity	[11]
NiCo oxide NPs/Ni	2 mA cm^{-2}	9	130 ppm NH_3 **+ 0.1M Na_2SO_4**	98% removal. 80% **NO_3^-** selectivity	[11]
$Ni(OH)_2$/NF	1.6 V_{RHE} (~6 mA cm^{-2})[e]	11.3[f]	0.2 M NH_3 **+ 0.1 M Na_2SO_4**	**$FE_{(N2)}$ 51%**	This work
$Ni(OH)_2$/NF	1.9 V_{RHE} (~30.5 mA cm^{-2})[e]	11.5[f]	0.3 M NH_3 **+ 0.1 M K_2SO_4**	**$FE(NO_3^-)$ 72%**[g]	This work
$Ni(OH)_2$/NF	1.6 V_{RHE} (~10 mA cm^{-2})[e]	13[f]	0.2 M NH_3 **+ 0.1 M NaOH**	**$FE(NO_2^-)$ 58%**	This work

[a] Nickel foam; [b] current is reported instead of current density; [c] CNT is carbon nanotubes; [d] CNS is carbon nanospheres; [e] Average current density in the first two hours of electrolysis. [f] Initial pH of the electrolyte. [g] Total FE in the end of 52h electrolysis.

Surface roughness of Ni foam

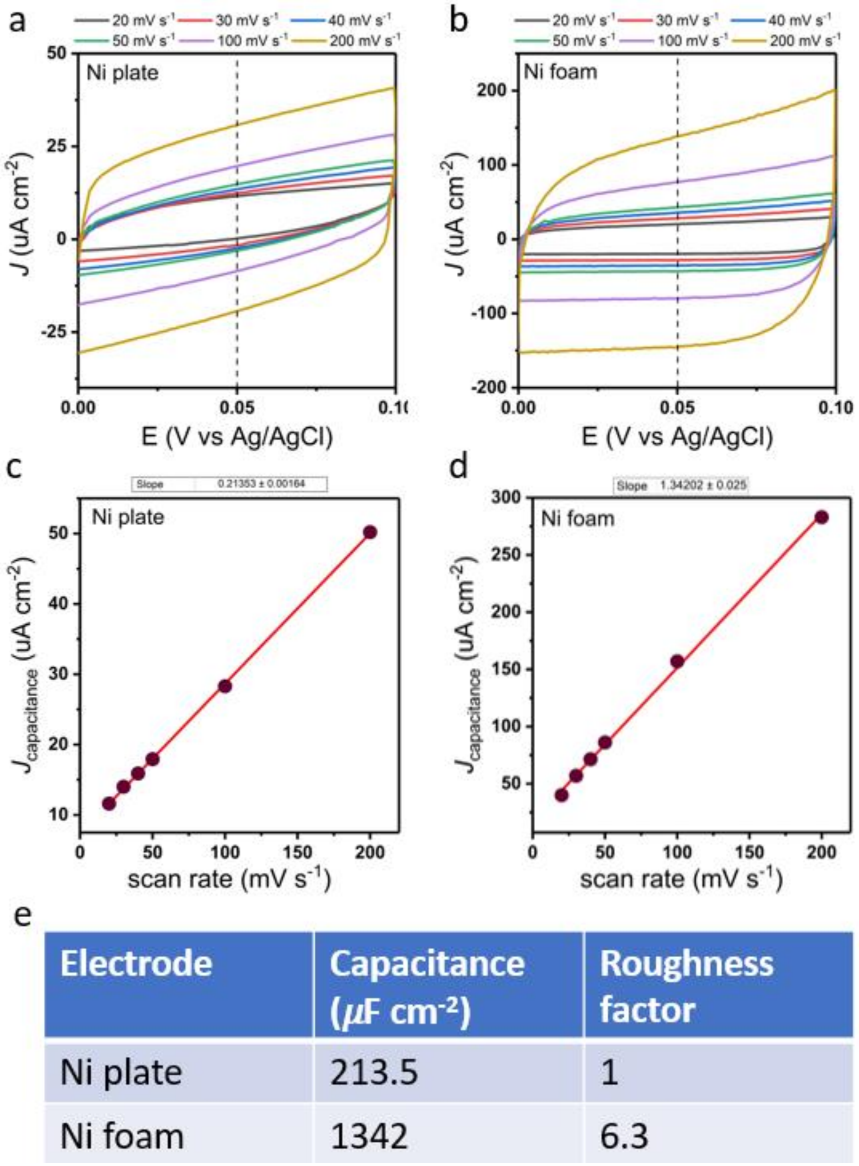

Electrode	Capacitance (μF cm^{-2})	Roughness factor
Ni plate	213.5	1
Ni foam	1342	6.3

Figure 2. Determination of double-layer capacitance Ni plate (a,c) and Ni foam (b,d) in 1M KOH (CVs taken over a range of scan rates; and currents due to double-layer charging plotted against scan rate). (e) Double-layer capacitance values and roughness factors of Ni materials.

Preparation of $Ni(OH)_2$/NF anode:

Ink preparation: Nanostructured $Ni(OH)_2$ catalyst was prepared using the optimized epoxide sol-gel synthesis method previously reported by our group.[12] Catalyst inks were made in a 15-ml glass vial by mixing of 120 mg of $Ni(OH)_2$ catalyst with 60 mg Vulcan Carbon Black (FuelCellStore) followed by the addition of 7 mL of absolute ethanol (>99.9% ACS grade, Sigma-Aldrich). The mixture was sonicated for a few seconds to disperse the powder in the solvent. Solution containing 0.6 mL of Nafion-117 solution (~5% in a mixture of lower aliphatic alcohols and water, Sigma-Aldrich) was added to the dispersed solution afterwards. Ink mixtures were then sonicated for 1 h at 60 ^{o}C in a closed vial.

Substrate preparation: Ni foam (1.6 mm thickness, MTI Corporation) was cut into several pieces with dimensions of 1 cm x 3 cm (width and length, respectively) for the standard electrode, and with dimensions of 1 cm x 6 cm for the electrode used in the preparative ammonia electrolysis. Nickel foam pieces were cleaned by successive sonication in acetone and water for 15 minutes, and then dried under Ar flow.

Anode preparation: Freshly cleaned Ni foam was immersed in the ink solution and sonicated for 10-15 minutes, pulled out and dried. Then the ink was dropcasted evenly onto both sides of the foam. The total volume of the ink deposited was adjusted to ~10 mg cm^{-2} of $Ni(OH)_2$ catalyst on each electrode. The as-prepared electrodes are shown in Figure S2:

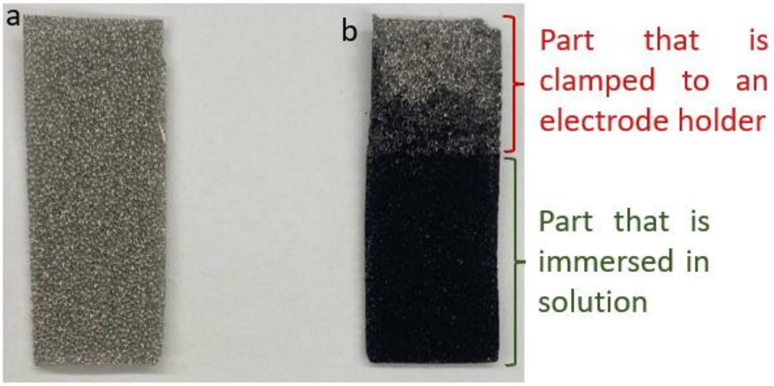

Figure S3. Photographs of a freshly cleaned Ni foam (a) and the prepared $Ni(OH)_2$/NF anode (b).

Electrochemical cell setup:

Cyclic voltammetry and chronoamperometry studies were conducted in a conventional gas-tight two-compartment cell (the volume of each compartment was 150 mL), equipped with an anion exchange (Fumasep FAB-PK-130, FuelCellStore), $Ni(OH)_2$/NF anode, NF cathode, and Ag/AgCl double-junction reference electrode and connected to an electrochemical workstation (Biologic SP-300). All recorded potentials (vs Ag/AgCl) were converted to the RHE scale using the Nernst equation: $E_{RHE} = E_{Ag/AgCl} + E^{o}_{Ag/AgCl} + 0.059 \times pH$, where $E^{o}_{Ag/AgCl} = 0.1976$ at 25 ^{o}C, and pH of the anolyte was measured using PH60 pH meter (APERA Instruments). All potentials are reported as measured, without Ohmic potential drop corrections. Ag/AgCl reference electrode was calibrated using 10mM ferro-ferricyanide system in 0.5 M H_2SO_4, and the obtained ox-red potentials agreed with those reported in the literature (Figure S12).[13]

0.1 M Na_2SO_4 (99%, ACP Chemicals) or 0.1 M NaOH (>97%, Sigma-Aldrich) solutions in Milli-Q water was used as catholyte and anolyte (the volume of the electrolyte in each compartment was 65 ml). NH_3-containing anolyte was prepared by the dilution of the concentrated solution of NH_3 (ACS reagent, 28-30% NH_3 basis, Sigma-Aldrich), the ammonia content in which was determined by ion chromatography (IC) using Metrohm Eco IC equipped with a cation column using 1.7 mM HNO_3 (ACS reagent, 70%, Sigma-Aldrich) + 1.7 mM 2,6-pyridinedicarboxylic acid (99%, Sigma-Aldrich) solution in Milli-Q water as an eluent. The calibration curve standards, containing 1-10 ppm NH_4^+ were prepared from NH_4F (>99.99%, Sigma-Aldrich).

Preparative electrolysis:

Preparative AOR was performed in a 150 ml divided cell equipped with inlet and outlet for the electrolyte circulation, 5 cm^2 $Ni(OH)_2$/NF anode, NF cathode, and Ag/AgCl single-junction reference electrode and connected to an electrochemical workstation (Biologic SP-50). 0.1 M K_2SO_4 (>99%, Sigma-Aldrich) or 0.1 M K_2HPO_4 (>98%, Sigma-Aldrich) with 0.2-0.3 M NH_3 solutions were used as an anolyte. 0.1 M K_2SO_4 or 1 M KOH (>85%, ACS reagent, Sigma-Aldrich) solutions were used as a catholyte. The volume of the electrolyte in each compartment was 145 ml, the flow rate of the electrolyte was 50 ml min^{-1}. Unless otherwise stated, electrolysis was stopped when current became low, and the total charge passed was close to the charge theoretically required for the full conversion of ammonia.

Product analysis:

In a course of potentiostatic electrolysis, Ar (99.999%, Praxair) was continuously bubbled through the reaction mixture at 10 mL min^{-1}. Ultra high purity Ar (99.999%, Praxair) was used in all experiments to minimize the amount of O_2 and N_2 originating from the carrier gas. Prior to the electrolysis, the system was purged with Ar during 1 h until GC showed only trace amount of O_2 and N_2, which then were used as a baseline. The gas products (N_2 and O_2) formed in a course of electrolysis were analyzed by gas chromatography (GC) using SRI MG-5 multiple gas analyzer connected to the cell through the ammonia trap containing 1 M H_2SO_4 solution (~ 100 ml glass tube equipped with septa, containing ~20 ml of acidic solution), preventing the NH_3 vapour getting into the GC columns and possible damaging of the instrument. Nitrate and nitrite concentrations were determined by ion chromatography (IC) using Metrohm Eco IC equipped with an anion column using 3.2 mM Na_2CO_3 (>99.5%, ACP Chemicals) + 1 mM $NaHCO_3$ (>99.7% VWR) solution in Milli-Q water as an eluent. The calibration curve standards, containing 1-10 ppm NO_3^-/NO_2^- were prepared from the commercially available solutions of these anions (1000 ppm, Sigma-Aldrich). The samples for IC were prepared by 100-times dilution of the reaction mixture (100 ul of the reaction mixture was taken from the cell for each measurement).

Calculation of faradaic efficiency of O_2 and N_2 formation:

The quantitative analysis of O_2 and N_2 was performed using a thermal conductivity detector (TCD). The Faradaic efficiency (FE) of the gas products was calculated[14] as:

$$FE\ (\%) = \frac{n_i \times F \times \Phi_i \times \mathrm{F}_m}{I} \quad \text{(S5)},$$

where $\mathbf{n_i}$ is a number of the transferred electrons ($\mathbf{n_i}$ = 4 for O_2 and 6 for N_2), **F** is the Faraday constant, $\mathbf{\Phi_i}$ is the volume fraction of the gas product being quantified (calculated by calibrating the GC data using a diluted mixture of the gases of known concentrations), **I** is the current value at the beginning of the measurement, $\mathbf{F_m}$ is the molar Ar gas flow rate.

Calculation of faradaic efficiency of nitrite and nitrate formation:

The quantitative analysis of nitrate and nitrite was performed using an ionic conductivity detector. The FE of the gas products was calculated as:

$$FE = \frac{n_i \times V \times C \times F}{Q \times M_w} \quad \text{(S6)},$$

where $\mathbf{n_i}$ is a number of the electrons transferred ($\mathbf{n_i}$ = 6 for NO_2^- and 8 for NO_3^-), **F** is the Faraday constant, **C** is the concentration of nitrate/nitrate in the analyte in *ppm*, **V** is the total volume of the anolyte, Q is the total charge passed, and $\mathbf{M_w}$ is the molecular weight of nitrate/nitrate.

Electrochemical impedance spectroscopy:

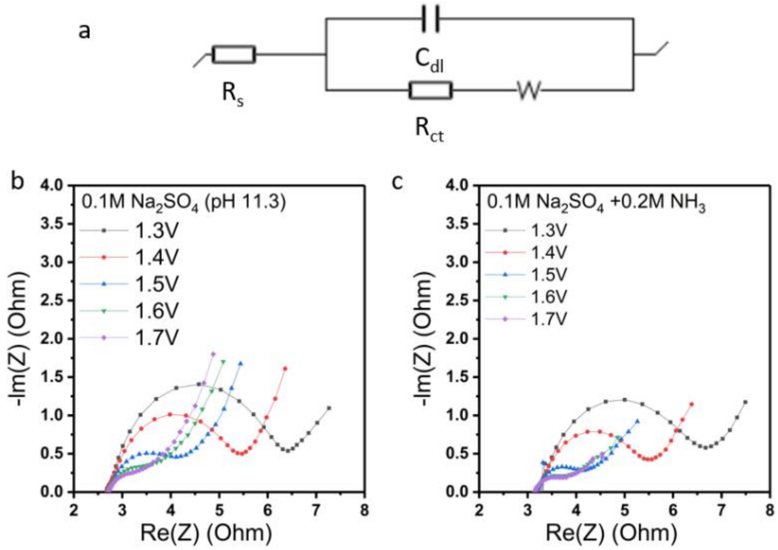

Figure S4. Nyquist impedance spectra recorded for the $Ni(OH)_2$/NF anode during the OER (b) or AOR (c) at different potentials. (a) A Randles circuit used for the interpretation of impedance spectra, consisting of the resistance of solution, double layer capacitance at the surface of the electrode as well as charge transfer resistance. Data are summarized in Table S4.

Table S4. Optimum fit parameters for the impedance date of Ni(OH)2/NF electrode in OER (0.1M Na_2SO_4) and AOR (0.1M Na_2SO_4 + 0.2M NH_3) systems, where R_s is solution resistance, C_{dl} is double layer capacitance at the surface of the electrode, R_{ct} is charge transfer resistance, and W is Warburg resistance.

E (V vs RHE)	Reaction	R_s (Ohm)	C_{dl} (mF)	R_{ct} (Ohm)	W (Ohm $s^{-1/2}$)
1.3	OER	2.761	1.59	3.136	1.037
1.4	OER	2.762	1.62	2.227	1.205
1.5	OER	2.775	2.43	1.142	1.349
1.6	OER	2.772	2.83	0.727	1.353
1.7	OER	2.775	2.51	0.548	1.394
1.3	AOR	3.302	1.62	2.792	1.124
1.4	AOR	3.297	1.494	1.856	1.016
1.5	AOR	3.245	1.987	0.845	0.907
1.6	AOR	3.225	2.705	0.602	0.739
1.7	AOR	3.21	3.108	0.561	0.592

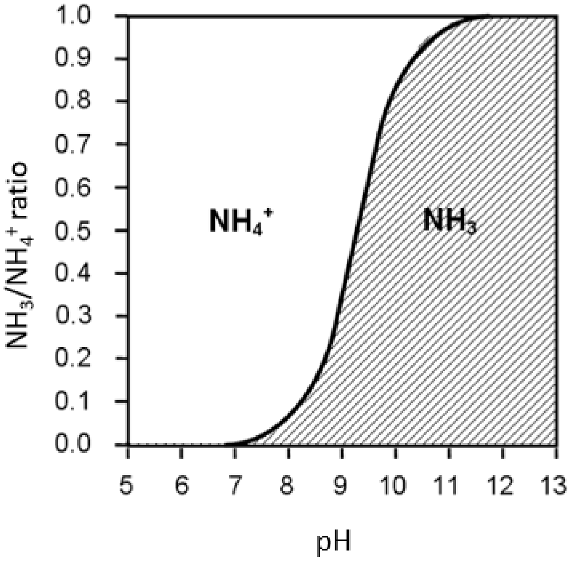

Figure S5. Ammonia to ammonium molecular ratio as a function of solution pH.

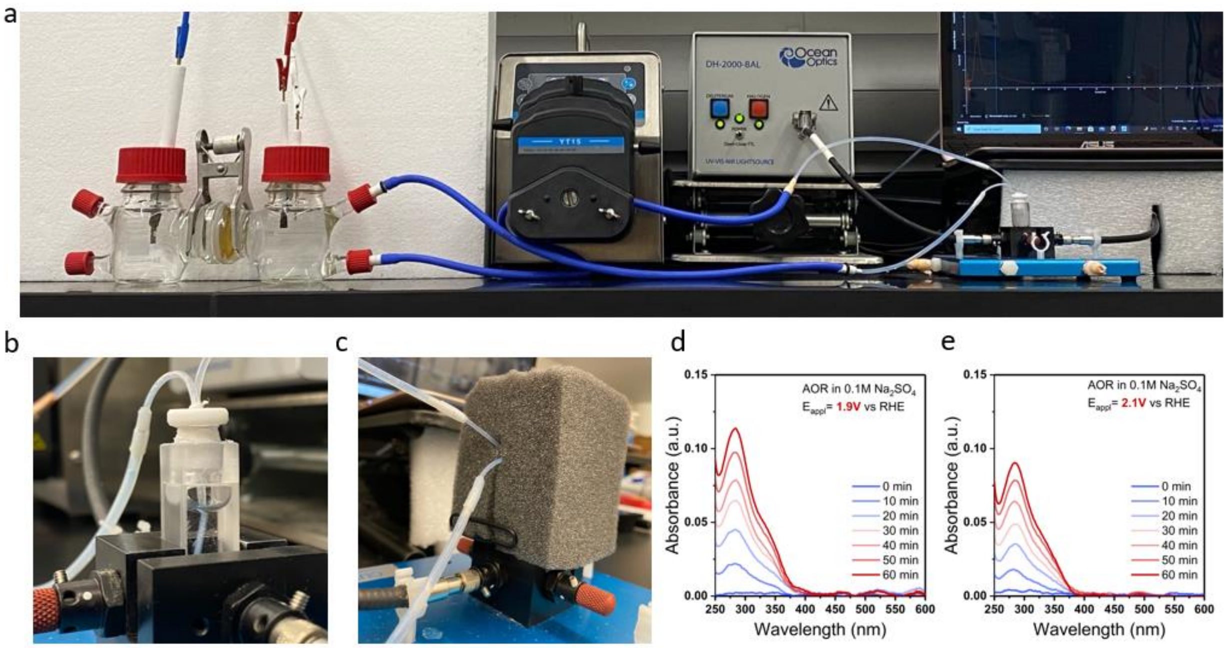

Figure S6. (a) Setup used for in-operando UV-Vis analysis of nitrate in a course if potentiostatic electrolysis of 0.2 M ammonia in 0.1 M Na_2SO_4 comprising of the following parts (from left to right): (1) divided electrochemical cell, connected to a potentiostat; (2) peristaltic pump; (3) UV-Vis spectrometer; (4) a cuvette. Peristaltic pump is used for the circulation of the anolyte through the cuvette. (b) close-up photo of the uncovered cuvette. (c) close-up photo of the covered cuvette. (d,e) examples of UV-Vis spectra recorded with 10-minute intervals in the course of AOR at 1.9 V (d) and 2.1 V (e).

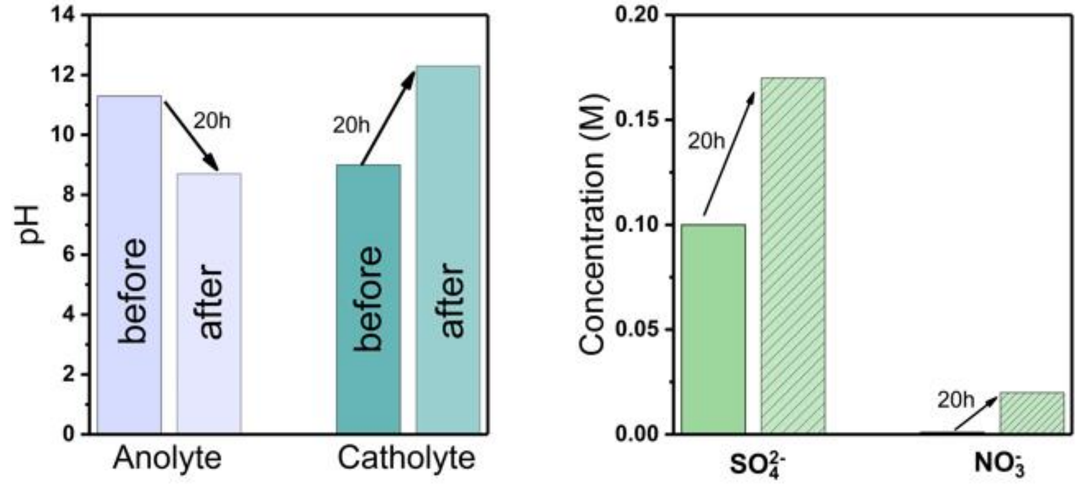

Figure S7. The pH changes in the catholyte and anolyte after 20 h electrolysis (left). The changes in SO_4^{2-} and NO_3^- concentrations in anolyte after 20 h electrolysis (right). Electrolysis was performed using NF cathode and 1.5 cm^2 $Ni(OH)_2$/NF anode using 0.1 M Na_2SO_4 as electrolyte for both compartments.

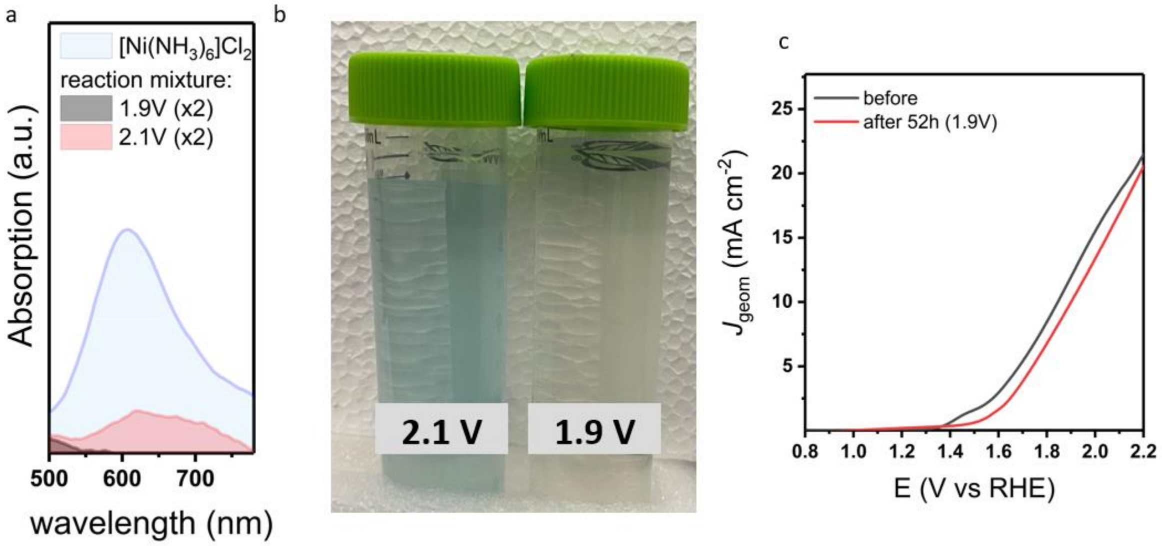

Figure S8. (a) UV-Vis spectra of aqueous [Ni(NH$_3$)$_6$]Cl$_2$, and reaction mixtures after the preparative electrolysis of 0.3 M NH$_3$ in 0.1 M Na$_2$SO$_4$ at 1.9 V and 2.1 V. (b) Photos of the solutions after the preparative electrolysis. (c) LSV curves recorded at 1 mV s^{-1} scan rate at Ni(OH)$_2$/NF catalyst (before the preparative electrolysis) and after for 0.2 M NH$_3$ + 0.1 M Na$_2$SO$_4$ solution.

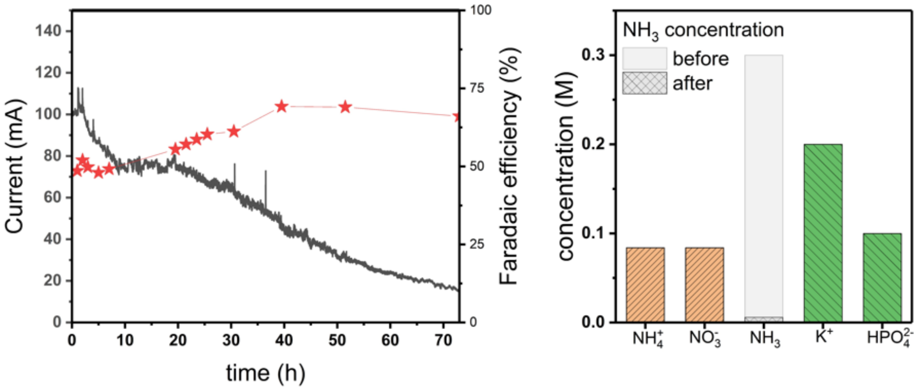

Figure S9. Preparative electrolysis of 0.3 M ammonia in 0.1 M K$_2$HPO$_4$ performed at 1.9 V vs RHE (left) and the anolyte composition after the electrolysis (right). Grey bars correspond to the NH$_3$ concentration before and after electolysis. Other bars represent the concentrations of ions after the electrolysis. Electrolysis was performed using 5 cm^2 Ni(OH)$_2$/NF anode.

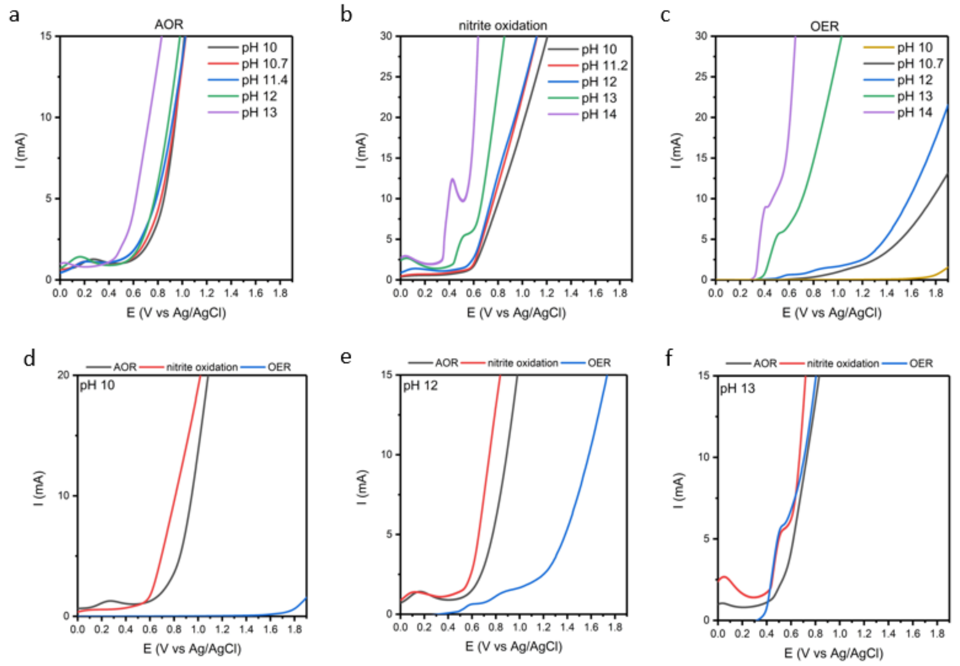

Figure S10. The effect of pH on the AOR, OER, and nitrite oxidation at Ni(OH)$_2$/NF anode. (a-c) LSV recorded at 10 mV s^{-1} at Ni(OH)$_2$/NF in 0.1 M Na$_2$SO$_4$, containing 0.2 M NH$_3$/NH$_4^+$ (a), 0.1 M NaNO$_2$ (b), and without any additives (c). Electrolytes with pH 9-12 were prepared by adjusting pH of the electrolyte by the addition of sulfuric acid or sodium hydroxide. For the reactions at pH 13 and 14, 0.1 M NaOH and 1 M NaOH were used as electrolytes. (d-e) Relative activity of AOR, nitrite oxidation, OER at Ni(OH)$_2$/NF anode at different pH: 10 (d), 12 (e), 13 (f).

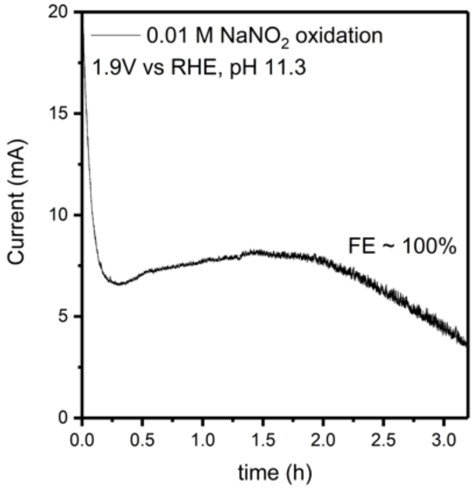

Figure S11. Electrolysis of 0.01 M NaNO$_2$ in 0.1 M Na$_2$SO$_4$ at 1.9 V vs RHE and pH 11.3 (pH was adjusted by adding an appropriate amount of NaOH).

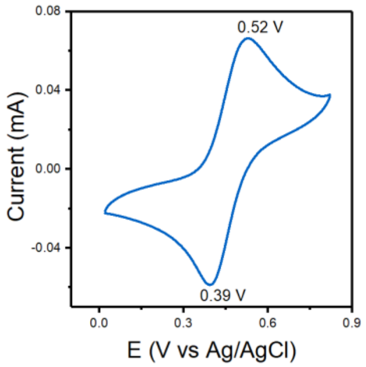

Figure S12. CV of 10 mM $K_2[Fe(CN)_6]$, recorded at scan rate 100 mV s^{-1} at glassy carbon electrode in in 0.5 M H_2SO_4 as supporting electrolyte. The half-wave potential ($E_{1/2}$) of the ferro-ferricyanide system was determined according to the following equation: $E_{1/2} = E_{pa} – 1/2\Delta E_p$, where Epa is the anodic peak potential, and ΔEp is the anodic and cathodic peak separation.

References:

1. E-commerce of chemical. https://www.echemi.com (assessed August 2021)
2. Independent Data & Analysis on Commodities and Production Processes. https://www.intratec.us (assessed August 2021)
3. A. Allagui, S. Sarfaz, S. Ntais, F. Al momani, E.A. Baranova, *Int. J. Hydr. Energy*, 2014, ***39***, 41–48.
4. Y.-J. Shin, W.-H. Huang, C.P. Huang, *Electrochim. Acta*, 2018, ***263***, 261-271.
5. A. Kapalka, A. Cally, S. Neodo, C. Comninellis, M. Wächter, K.M. Udert, *Electrochem. Commun.*, 2010, ***12***, 18–21.
6. R. Wang, H. Liu, K. Zhang, G. Zhang, H. Lan, J. Qu, *Chem. Eng. J.*, 2021, ***404***, 126795.
7. X. Jiang, D. Ying, X. Liu, M. Liu, S. Zhou, C. Guo, G. Zhao, Y. Wang, J. Jia, *Electochim. Acta*, 2020, ***345***, 136157.
8. M. Gonzalez-Reyna, M.S. Luna-Martínez, J.F. Perez-Robles, *Nanotechnology*, 2020, ***31***, 235706.
9. M.-H. Tsai, T.-C. Chen, Y. Juang, L.-C. Hua, C. Huang, *Electrochem. Commun.*, 2020, ***121***, 106875.
10. F. Almomani, R. Bhosale, M. Khraisheh, A. Kumar, M. Tawalbeh, *Int. J. Hydr. Energy*, 2020, ***45***, 10398–10408
11. Y.-J. Shin, C.-H. Hsu, *Chem. Eng. J.*, 2021, ***409***, 128024.
12. S. W. Tatarchuk, R. M. Choueiri, X. V. Medvedeva, L. D. Chen, A. Klinkova, *Chemosphere* **2021**, *279*, 130550.
13. A.F. Azevedo, M.R. Baldan, N.G. Ferreira, *Int. J. Electrochem.*, 2012, 508453.
14. R. Kas, R. Kortlever, A. Mibrat, M. T. M. Koper, G. Mul, J. Baltrusaitis, *Phys. Chem. Chem. Phys*. 2014, ***16***, 12194-12201.